Self-Association and DNA-Binding Properties of Two Triple Helix-Specific Ligands: Comparison of a Benzo[e]pyridoindole and a Benzo[g]pyridoindole

Daniel S. Pilch,*,†,‡ Marie-Thérèse Martin,§ Chi Hung Nguyen,∥ Jian-Sheng Sun,† Emile Bisagni,∥ Thérèse Garestier,† and Claude Hélène†

Contribution from the Laboratoire de Biophysique, Muséum National d'Histoire Naturelle, INSERM U 201, CNRS URA 481, 43 rue Cuvier, 75231 Paris Cedex 05, France, the Laboratoire de Chimie, Muséum National d'Histoire Naturelle, CNRS URA 401, 63 rue Buffon, 75231 Paris Cedex 05, France, and the Laboratoire de Synthèse Organique, Institut Curie-Biologie, CNRS URA 1387, Bâtiment 110, 91405 Orsay, France

Received April 23, 1993®

Abstract: The self-association and DNA-binding properties of two benzopyridoindole derivatives, 3-methoxy-7*H*-8-methyl-11-[(3′-aminopropyl)amino]benzo[*e*]pyrido[4,3-*b*]indole (BePI) and 3-methoxy-7-[((3′-diethylamino)propyl)-amino]-10-methyl-11*H*-benzo[*g*]pyrido[4,3-*b*]indole (BgPI), have been investigated by a variety of NMR, spectrophotometric, fluorescence, and hydrodynamic techniques. NMR studies indicate that both BePI and BgPI self-associate in solution, probably forming multimers (*n*-mers) in the process. BgPI self-associates with a 3-fold (at 80 °C) to 12-fold (at 27 °C) higher affinity than BePI. Self-association interactions do not interfere with those between either ligand and DNA at total ligand concentrations $\leq 10^{-5}$ M. Thermodynamic (van't Hoff) analyses of the self-association interactions of both ligands indicate that they are enthalpically driven, consistent with those of other aromatic dyes. Furthermore, at temperatures ranging from 22 to 80 °C, BgPI self-associated complexes are 1.2–1.5 kcal/mol more stable than the corresponding BePI self-associated complexes. The solvent exchange properties of the exchangeable protons of both BePI and BgPI, as determined by NMR studies in H_2O at [multimer]/[monomer] ratios of ≈ 4, reveal exchange in the following order as a function of either pH or temperature: 10-NH > 11-NH $\gg$ 7-NH $\gg$ 3′-NH for BePI and 8-NH > 7-NH $\gg$ 11-NH $\gg$ 3′-NH for BgPI (see Figure 1 for numbering systems of atoms). These studies also suggest that stacking interactions between heterocyclic ring portions of neighboring molecules are involved in the self-association process. Thermal denaturation studies demonstrate that both BePI and BgPI preferentially bind and stabilize triple-helical relative to double-helical DNA, the latter ligand doing so to a greater extent than the former. Binding to either double-helical or triple-helical polydeoxynucleotides quenches the fluorescence of both ligands, with the greatest degree of quenching accompanying binding to triplex relative to duplex DNA. In addition, binding to either duplex or triplex DNA quenches the fluorescences of BgPI to a substantially greater extent than that of BePI. Viscosity studies are consistent with the conclusion that both ligands bind DNA by intercalation.

Introduction

Recent evidence demonstrating the therapeutic potential of oligonucleotide-directed triplex formation[1,2] and suggesting that intramolecular triple helixes may play important biological roles *in vivo*[3] has generated a great deal of interest in the triple-helical form of nucleic acids. The therapeutic potential of oligonucleotide-directed triplex formation in applications involving the control of gene expression has been highlighted by the work of several groups.[4-10] These applications may include strategies aimed at inhibiting either transcription,[4,7-9,10] DNA replication[5,11] or cellular protein binding to designated DNA targets.[12-14]

Thermodynamic studies have indicated that triplexes are generally less stable than the corresponding duplexes.[15-18] Strategies aimed at enhancing triplex stability should therefore enhance the therapeutic potential of triplex formation. Various strategies have been explored thus far, including the tethering of intercalating agents to the ends of third-strand oligonucleotides[19,20] and

* Author to whom correspondence should be addressed.
† Laboratoire de Biophysique, Muséum National d'Histoire Naturelle.
‡ Present address: Department of Chemistry, Wright-Rieman Laboratories, Rutgers—The State University of New Jersey, P.O. Box 939, Piscataway, NJ 08855-0939.
§ Laboratoire de Chimie, Muséum National d'Histoire Naturelle.
∥ Laboratoire de Synthèse Organique, Institut Curie-Biologie.
® Abstract published in *Advance ACS Abstracts*, October 1, 1993.

(1) Hélène, C. *Anti-Cancer Drug Des.* **1991**, *6*, 569–584.
(2) Hélène, C. *Eur. J. Cancer* **1991**, *27*, 1466–1471.
(3) Wells, R. D.; Collier, D. A.; Hanvey, J. C.; Shimizu, M.; Wohlrab, F. *FASEB J.* **1988**, *2*, 2939–2949.
(4) Cooney, M.; Czernuszewicz, G.; Postel, E. H.; Flint, S. J.; Hogan, M. E. *Science* **1988**, *241*, 456–459.
(5) Birg, F.; Praseuth, D.; Zerial, A.; Thuong, N. T.; Asseline, U.; Le Doan, T.; Hélène, C. *Nucleic Acids Res.* **1990**, *18*, 2901–2908.
(6) Orson, F. M.; Thomas, D. W.; McShan, W. M.; Kessler, D. J.; Hogan, M. E. *Nucleic Acids Res.* **1991**, *19*, 3435–3441.
(7) Young, S. L.; Krawczyk, S. H.; Matteucci, M. D.; Toole, J. J. *Proc. Natl. Acad. Sci. U.S.A.* **1991**, *88*, 10023–10026.
(8) Duval-Valentin, G.; Thuong, N. T.; Hélène, C. *Proc. Natl. Acad. Sci. U.S.A.* **1992**, *89*, 504–508.
(9) Grigoriev, M.; Praseuth, D.; Robin, P.; Hemar, A.; Saison-Behmoaras, T.; Dautry-Varsat, A.; Thuong, N. T.; Hélène, C.; Harel-Bellan, A. *J. Biol. Chem.* **1992**, *267*, 3389–3395.
(10) Postel, E. H.; Flint, S. J.; Kessler, D. J.; Hogan, M. E. *Proc. Natl. Acad. Sci. U.S.A.* **1991**, *88*, 8227–8231.
(11) Giovannangeli, C.; Thuong, N. T.; Hélène, C. *Proc. Natl. Acad. Sci. U.S.A.* **1993**, submitted.
(12) Maher, L. J., III; Wold, B.; Dervan, P. B. *Science* **1989**, *245*, 725–730.
(13) François, J. C.; Saison-Behmoaras, T.; Thuong, N. T.; Hélène, C. *Biochemistry* **1989**, *28*, 9617–9619.
(14) Hanvey, J. C.; Shimizu, M.; Wells, R. D. *Nucleic Acids Res.* **1990**, *18*, 157–161.
(15) Pilch, D. S.; Brousseau, R.; Shafer, R. H. *Nucleic Acids Res.* **1990**, *18*, 5743–5750.
(16) Plum, G. E.; Park, Y. W.; Singleton, S. F.; Dervan, P. B.; Breslauer, K. J. *Proc. Natl. Acad. Sci. U.S.A.* **1990**, *87*, 9436–9440.
(17) Manzini, G.; Xodo, L. E.; Gasparotto, D.; Quadrifoglio, F.; van der Marel, G. A.; van Boom, J. H. *J. Mol. Biol.* **1990**, *213*, 833–843.
(18) Rougée, M.; Faucon, B.; Mergny, J. L.; Barcelo, F.; Giovannangeli, C.; Garestier, T.; Hélène, C. *Biochemistry* **1992**, *31*, 9269–9278.
(19) Sun, J. S.; François, J. C.; Montenay-Garestier, T.; Saison-Behmoaras, T.; Roig, V.; Thuong, N. T.; Hélène, C. *Proc. Natl. Acad. Sci. U.S.A.* **1989**, *86*, 9198–9202.

0002-7863/93/1515-9942$04.00/0

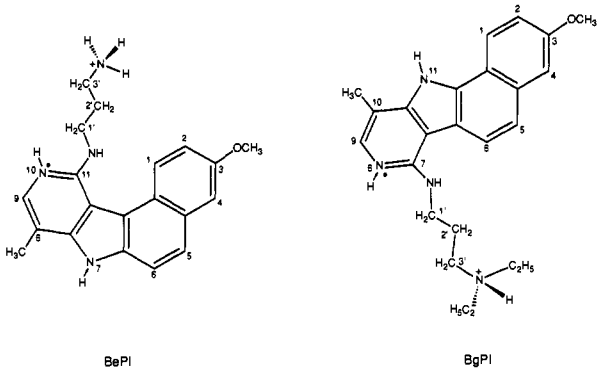

Figure 1. Structures of BePI {3-methoxy-7*H*-8-methyl-11-[(3′-aminopropyl)amino]benzo[*e*]pyrido[4,3-*b*]indole} (left) and BgPI {3-methoxy-7-[(3′-diethylamino)propyl)amino]-10-methyl-11*H*-benzo[*g*]pyrido[4,3-*b*]indole} (right), indicating the atomic numbering systems.

photoinduction of covalent cross-links between the third strand and the underlying duplex via a tethered photoactivatable agent.[21,22] Another approach involves the use of triplex-specific ligands, which, upon binding, markedly stabilize triple-helical structures. One such family of ligands, the benzopyridoindoles, has been investigated recently.[23-25] The triplex-stabilizing effects of these ligands are not restricted to triplexes containing solely T×A·T (× = Hoogsteen base pairing) base triplets,[23-25] contrasting the results obtained from studies probing the interactions of the intercalator, ethidium bromide (EtBr), with triple-helical DNA.[26-29] One of the benzopyridoindoles, BePI (Figure 1, left), was shown to increase significantly the extent of transcriptional inhibition *in vitro* by oligonucleotide-directed triplex formation.[24] Furthermore, this ligand was shown to intercalate into both double-helical and triple-helical DNA.[25]

When evaluating the nucleic acid-binding properties of a ligand, it is important to consider its potential for self-association. Should a ligand be shown to self-associate, the implications of self-association on interactions between the ligand and nucleic acid targets must be taken into account. In this work, we investigate the self-association and DNA-binding properties of two structurally distinct benzopyridoindoles, BePI and BgPI. NMR studies demonstrate that both ligands self-associate in solution, with BgPI having a 3-fold (at 80 °C) to 12-fold (at 27 °C) higher self-affinity than BePI. Thermodynamic analysis reveals that the self-association interactions are enthalpically driven. Exchangeable proton NMR experiments suggest that stacking interactions are involved in the self-association process. Helix–coil transition profiles demonstrate that both BePI and BgPI preferentially bind and stabilize triplex relative to duplex DNA. Binding to DNA quenches the fluorescence of both ligands significantly, the extent of which is greater upon binding to triplex relative to duplex DNA. Furthermore, the extent of quenching is significantly greater in BgPI/DNA relative to BePI/DNA complexes. Viscosity studies suggest that both ligands bind DNA by intercalation.

Experimental Section

Polydeoxynucleotides, Ligands, and Other Reagents. Poly(dA), poly(dT), poly[d(A-T)]·poly[d(A-T)] {poly[d(A-T)$_2$]}, and poly[d(G-C)]·poly[d(G-C)] {poly[d(G-C)$_2$]} were obtained from Pharmacia P-L Biochemicals Inc. Polymers were dissolved to concentrations of approximately 7 mM in nucleotide with 10 mM sodium cacodylate (pH 7.0). Concentrations of all DNA polymers were determined spectrophotometrically using the following extinction coefficients in units of (mol of nucleotide/L)$^{-1}$ cm^{-1}: ϵ_{257nm} = 8600 for poly(dA), ϵ_{265nm} = 8700 for poly(dT), ϵ_{262nm} = 6600 for poly[d(A-T)$_2$], and ϵ_{254nm} = 8400 for poly[d(G-C)$_2$]. Solutions containing either the poly(dA)·poly(dT) duplex or the poly(dT)×poly(dA)·poly(dT) [poly(dA)·2poly(dT)] triplex were prepared by mixing poly(dA) and poly(dT) at either 1:1 or 1:2 molar ratios, respectively, heating to 90 °C in a water bath, and then cooling to room temperature.

BePI and BgPI were synthesized as reported previously by Bisagni and co-workers.[30] Extinction coefficients for both ligands were determined from the absorbance spectra of 6 μM ligand solutions containing 10 mM sodium cacodylate (pH 6.0), 300 mM NaCl, and 0.1 mM EDTA (CNE buffer) and are as follows in units of (mol/L)$^{-1}$ cm^{-1}: ϵ_{361nm} = 5500 for BePI and ϵ_{352nm} = 5300 for BgPI. Under these conditions, both ligands are in their fully protonated (doubly-charged, 2+) monomeric states. Deprotonation of these ligands alters their spectrophotometric properties. Hence, changes in pH may induce corresponding changes in the extinction coefficients of these ligands. All other buffer reagents were obtained from Sigma Chemical Co.

Thermal Denaturation Experiments. All thermal denaturation studies were carried out in CNE buffer on a Uvikon 940 spectrophotometer, interfaced to an IBM-AT personal computer for data collection and analysis. Temperature control of the cell holder was maintained by a Haake P2 circulating water bath. The temperature of the water bath was raised from 35 to 95 °C at a rate of 0.10 °C/min by a Haake PG 20 thermoprogrammer, and the absorbance at 260 nm was recorded every 7 min. All the thermal denaturation profiles were reversible to within ±2 °C. Experimental solutions contained poly(dA)·2poly(dT) at a concentration of 40 μM base triplet and either BePI or BgPI at concentrations of either 0, 1.3, 4, or 8 μM. It should be pointed out that melting profiles acquired in CNE buffer showed no evidence of disproportionation of poly(dA)·poly(dT) into triplex [poly(dA)·2poly(dT)] and single-stranded [poly(dA)] forms.

Static Fluorescence Measurements. All static fluorescence measurements were carried out on a SPEX Fluorolog F1T11T spectrofluorimeter, and the cell holder was maintained at a constant temperature of 25 °C with a Huber Ministat circulating water bath. Fluorescence emission spectra of solutions containing either BePI or BgPI at a concentration of 1.5 μM and either poly(dA)·poly(dT), poly(dA)·2poly(dT), poly[d(A-T)$_2$], or poly[d(G-C)$_2$] at concentrations of either 0 or 21 μM base pair or base triplet ([base pair or base triplet]/[ligand] = 14) were measured from either 370 to 560 nm for BePI-containing solutions or 340 to 525 nm for BgPI-containing solutions. The excitation wavelength was 315 nm for the BePI-containing solutions and 280 nm for the BgPI-containing solutions. For all samples, the excitation pathlength was 0.2 cm, while the emission pathlength was 1 cm. The excitation and emission spectral resolutions were 3.25 and 6.5 nm, respectively. Emission spectra were corrected to reflect an equal number of absorbed photons at the given excitation wavelength.

Viscosity Experiments. Viscosity measurements were carried out in a simple capillary viscometer[31] submerged in a water bath which was maintained at 24.5 ± 0.1 °C. Flow times were measured in triplicate to an accuracy of ±0.1 s with a stopwatch, and the average time of the different replicates was used. Viscosity studies on the plasmid, pBR322, were conducted in buffer containing 10 mM tris·HCl (pH 7.0) and 1 mM EDTA. Aliquots (1–8 μL) of either BePI or BgPI solutions (600 μM) were titrated directly into the viscometer containing a solution (1 mL) of 150 μM nucleotide pBR322, and flow times in the range 98–110 s were measured after each addition.

^{1}H NMR Measurements. All NMR experiments were carried out on a 300-MHz Bruker ACP 300 spectrometer, equipped with an Oxford Instruments magnet and an Aspect 3000 computer. Exchangeable proton

(20) Sun, J. S.; Giovannangeli, C.; François, J. C.; Kurfurst, R.; Montenay-Garestier, T.; Asseline, U.; Saison-Behmoaras, T.; Thuong, N. T.; Hélène, C. *Proc. Natl. Acad. Sci. U.S.A.* **1991**, *88*, 6023–6027.
(21) Takasugi, M.; Guendouz, A.; Chassignol, M.; Decout, J. L.; Lhomme, J.; Thuong, N. T.; Hélène, C. *Proc. Natl. Acad. Sci. U.S.A.* **1991**, *88*, 5602–5606.
(22) Giovannangeli, C.; Thuong, N. T.; Hélène, C. *Nucleic Acids Res.* **1992**, *20*, 4275–4281.
(23) Mergny, J. L. Ph.D. Thesis, Université Paris VI, 1991, pp 95–104.
(24) Mergny, J. L.; Duval-Valentin, G.; Nguyen, C. H.; Perrouault, L.; Faucon, B.; Rougée, M.; Montenay-Garestier, T.; Bisagni, E.; Hélène, C. *Science* **1992**, *256*, 1681–1684.
(25) Pilch, D. S.; Waring, M. J.; Sun, J. S.; Rougée, M.; Nguyen, C. H.; Bisagni, E.; Garestier, T.; Hélène, C. *J. Mol. Biol.* **1993**, *232*, in press.
(26) Lehrman, E.; Crothers, D. M. *Nucleic Acids Res.* **1977**, *4*, 1381–1392.
(27) Lee, J. S.; Johnson, D. A.; Morgan, A. R. *Nucleic Acids Res.* **1979**, *6*, 3073–3091.
(28) Scaria, P. V.; Shafer, R. H. *J. Biol. Chem.* **1991**, *266*, 5417–5423.
(29) Mergny, J. L.; Collier, D.; Rougée, M.; Montenay-Garestier, T.; Hélène, C. *Nucleic Acids Res.* **1991**, *19*, 1521–1526.
(30) Nguyen, C. H.; Lhoste, J. M.; Lavelle, F.; Bissery, M. C.; Bisagni, E. *J. Med. Chem.* **1990**, *33*, 1519–1528.
(31) Waring, M. J.; Henley, S. M. *Nucleic Acids Res.* **1975**, *2*, 567–586.

NMR measurements as a function of pH were conducted on 400 μL of solution (90% H_2O/10% D_2O) containing 10 mM sodium phosphate, 300 mM NaCl, and either 8.9 mM BePI or 7.5 mM BgPI. The starting pH values were 2.0 and 1.6 for the BePI and BgPI experiments, respectively. Aliquots (1–3 μL) of 1 N NaOH were added to each ligand solution, and the proton NMR spectrum and the solution pH were recorded after each addition. All pH values were measured directly in the NMR sample tubes with a MI-412 microelectrode (Microelectrodes, Inc.). The temperatures were fixed at 0 and 35 °C for the BePI and BgPI experiments, respectively. Exchangeable proton NMR measurements as a function of temperature were conducted on 400 μL of solution (90% H_2O/10% D_2O) containing 10 mM sodium phosphate (pH 5.0), 300 mM NaCl, and either 8.9 mM BePI or 7.5 mM BgPI. The $1\bar{3}3\bar{1}$ solvent suppression pulse sequence[32] was used to acquire all exchangeable proton NMR spectra, with the carrier frequency set on the H_2O resonance. The interval delay, τ, between pulses was 280 μs and the recycle delay was 1 s.

NMR studies probing the self-association of BePI and BgPI were carried out at pD 3.9 (pH meter reading of 3.5 plus 0.4 as a correction for the presence of D_2O[33]) on D_2O solutions (350 μL) containing 10 mM sodium phosphate, 300 mM NaCl, and either BePI or BgPI at concentrations ranging from 50 μM to 50 mM. NMR spectra were acquired at temperatures of either 22, 27, 35, 60, or 80 °C. In all cases, a recycle delay of 1 s was used.

Determination of K_a for Self-Association to Form n-Mers. A molecule, D, may self-associate in solution according to the following series of equilibria:

$$D + D \rightleftharpoons D_2$$

$$D_2 + D \rightleftharpoons D_3$$

$$\vdots$$

$$D_{n-1} + D \rightleftharpoons D_n$$

Dimicoli and Hélène[34] have previously derived the following equation relating changes in chemical shift of the NMR resonance corresponding to the proton under investigation as a function of the total concentration of D and the observed association constant, K_a:

$$\left(\frac{\Delta\delta}{D_T}\right)^{1/2} = \left(\frac{K_a}{2\Delta\delta_{D_2}}\right)^{1/2}(2\Delta\delta_{D_2} - \Delta\delta) \qquad (1)$$

where δ is the observed chemical shift, K_a is the association constant, D_T is the total concentration of D, $\Delta\delta = \delta_D - \delta$, and $\Delta\delta_{D_2} = \delta_D - \delta_{D_2}$. δ_D and δ_{D_2} are the chemical shifts of the resonances corresponding to the proton under investigation in either the monomeric (D) or dimeric (D_2) form of the molecule, respectively. Equation 1 is predicated on the following assumptions: First, successive association constants for each of the equilibria shown above are identical. Second, the effects of magnetic anisotropy from only neighboring molecules are considered, and these effects are additive. Third, the monomeric and self-associated species are in rapid exchange. Equation 1 indicates that plots of $(\Delta\delta/D_T)^{1/2}$ versus $\Delta\delta$ will be linear, and K_a may be derived from the slope (s) and x-intercept (x_0) of this plot ($K_a = x_0 s^2$). It should be pointed out that δ_D is obtained by extrapolation of the observed chemical shift to zero concentration. However, small changes in the extrapolated chemical shift do not significantly alter the values for K_a or δ_{D_2}.

Results and Discussion

Self-Association of BePI and BgPI. The chemical shifts of the aromatic proton resonances of both BePI and BgPI undergo marked downfield shifts ($\Delta\delta \approx$ 200–500 Hz) as the total ligand concentrations decrease from 50 mM to 50 μM. These chemical shift changes indicate that both BePI and BgPI self-associate in solution. Plots of $(\Delta\delta/D_T)^{1/2}$ versus $\Delta\delta$ for the aromatic protons of both BePI and BgPI at 27 °C are presented in Figure 2, parts A and B, respectively. Each of the plots is linear throughout the entire range of total ligand concentrations.

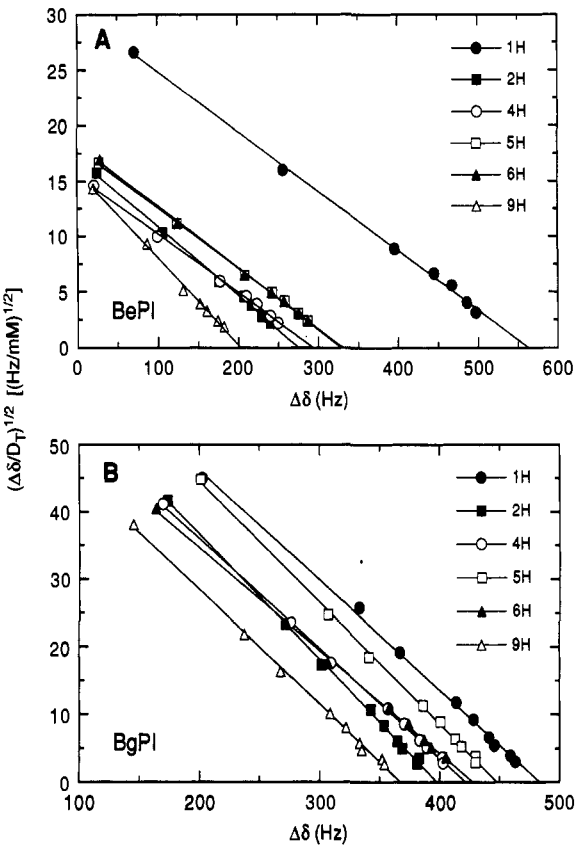

Figure 2. Plots of $(\Delta\delta/D_T)^{1/2}$ versus $\Delta\delta$ for the indicated aromatic protons of either BePI (A) or BgPI (B) at 27 °C in D_2O at pD = 3.9. Buffer conditions are 10 mM sodium phosphate and 300 mM NaCl. Total ligand concentrations range from 50 μM to 50 mM.

Pilch et al.[25] have previously shown by fluorescence and absorbance studies that BePI exists in its fully protonated (or deuterated in D_2O solutions), doubly-charged (2+) state at pH ≤ 6.0 (pD ≤ 6.4) when free and at pH ≤ 7.0 (pD ≤ 7.4) when bound to DNA. Separate studies (data not shown) on both free and DNA-bound BgPI indicate that it behaves similarly. The data presented in Figures 2, 3, and 4, as well as in Tables I and II, reflect experiments carried out at pD 3.9 (pH 3.5). However, control experiments (data not shown) at pD 5.4 (pH 5.0) yield virtually identical results, suggesting that similar results would be obtained throughout the pD range (pD ≤ 6.4) in which either BePI or BgPI remains fully deuterated (or protonated in H_2O solutions).

An equation similar to eq 1 applies to the dimerization of molecules.[34] Hence, plots of $(\Delta\delta/D_T)^{1/2}$ versus $\Delta\delta$ do not distinguish between dimerization and formation of n-mers. However, there is no reason to suppose that self-association of these ligand molecules should be limited to formation of dimers, and the large $\Delta\delta$ values are consistent with this notion. Thus, the plots in Figure 2 were analyzed with eq 1, and the average of the resulting association constants, as calculated for each of the aromatic protons, except the 1H proton of BePI (see below), was determined. These calculations yield self-association constants at 27 °C of 1.0 (±0.15) × 10^3 M^{-1} for BePI and 1.2 (±0.18) × 10^4 M^{-1} for BgPI (see Table I), indicating that BgPI has a higher self-affinity than BePI. This difference in self-affinity may arise from structural differences between the two molecules. The heterocyclic portion of BePI is crescent-shaped (curved), while that of BgPI is more linear (see Figure 1). Stacking interactions between neighboring molecules may be facilitated by the latter conformation through an enhanced degree of ring overlap relative to the former conformation. Furthermore, it is likely that the

(32) Hore, P. J. *J. Magn. Reson.* **1983**, *54*, 539–542.
(33) Glasoe, P. K.; Long, F. A. *J. Phys. Chem.* **1960**, *64*, 188–190.
(34) Dimicoli, J. L.; Hélène, C. *J. Am. Chem. Soc.* **1973**, *95*, 1036–1044.
(35) McGhee, J. D. *Biopolymers* **1976**, *15*, 1345–1375.

Table I. Effect of Temperature on the Self-Association of BePI and BgPI[a]

temp (°C)	$K_a \times 10^{-2}$ (M^{-1})[b]	$\Delta G°$ (kcal/mol)[c]
	BePI	
27	10 ± 1.5	−4.1 ± 0.1
35	6.5 ± 0.8	−4.0 ± 0.1
60	3.6 ± 0.5	−3.9 ± 0.1
80	2.2 ± 0.3	−3.8 ± 0.1
	BgPI	
22	190 ± 3.4	−5.8 ± 0.1
27	120 ± 18	−5.6 ± 0.1
35	65 ± 9.6	−5.4 ± 0.1
60	21 ± 3.4	−5.1 ± 0.1
80	7.4 ± 0.9	−4.6 ± 0.1

[a] Experiments were carried out at pD 3.9 in D_2O solutions containing 10 mM sodium phosphate and 300 mM NaCl. [b] Values represent the averages over those determined (according to eq 1) from $(\Delta\delta/D_T)^{1/2}$ vs $\Delta\delta$ plots for all of the aromatic protons, with the exception of the 1H proton of BePI. [c] Mol refers to mole of self-associated complex formed.

curved shape of the heterocyclic portion of BePI creates the potential for close-range, steric interactions between the aliphatic amino chain and the benzyl moiety, particularly at positions 1 and 2 (Figure 1, left). These interactions, which would be absent in BgPI molecules, might reduce the extent of stacking between neighboring BePI molecules by reducing ring overlap between benzyl moieties.

It is interesting to note that, while the slope of the $(\Delta\delta/D_T)^{1/2}$ versus $\Delta\delta$ plot for the 1H proton of BePI (figure 2A) is similar ($s \approx -0.054$ $Hz^{-1/2}$ $mM^{-1/2}$) to those for the other BePI aromatic protons, $\Delta\delta$ is substantially larger (by approximately 240–370 Hz) over the same range of concentrations. Hence, the association constant at 27 °C calculated for this plot with eq 1 was correspondingly high ($K_a = x_0 s^2 = 1.6 \times 10^3$ M^{-1}). As discussed above, the structure of BePI creates the potential for steric interactions between the 1H proton and the aliphatic amino chain. Moreover, the nature and/or presence of these interactions may differ in the self-associated and monomeric forms of BePI. Such differences would affect the chemical shift of the 1H proton, and thereby contribute to the comparatively large $\Delta\delta$. Thus, the changes in observed chemical shift for this proton would reflect more than just the type of self-association (stacking) interactions, which dictate the changes in the observed chemical shifts of the other aromatic protons. For this reason, the calculated K_a value for the 1H proton was not included in the group of K_a values over which the observed self-association constant of BePI was averaged.

While the chemical shifts of the resonances corresponding to the methyl, methoxy, and methylene protons of both BePI and BgPI also undergo downfield shifts as the total ligand concentrations decrease from 50 mM to 50 μM (data not shown), they generally do so to a lesser extent than do the aromatic protons. Conformational changes in the aliphatic amino chains upon self-association may induce larger changes in the chemical shifts of resonances corresponding to specific protons therein relative to others, as was observed, for example, for the 3′-CH_2 proton resonance of BePI (data not shown). In addition, the nature of the self-association (stacking) interactions may be such that the magnetic environments of the methyl and methoxy protons are differentially altered upon self-association. On account of these potential sources of variability in the $\Delta\delta$ values of the methyl, methoxy, and aliphatic amino chain protons, data corresponding to these protons were not averaged into the calculated self-association constants.

The positively-charged (2+) nature of both BePI and BgPI should induce repulsive rather than attractive electrostatic interactions. However, the charged character of these molecules should confer a substantial permanent dipole upon them as well. It is therefore likely that both dipolar and stacking interactions provide the driving forces for the self-association of these molecules.

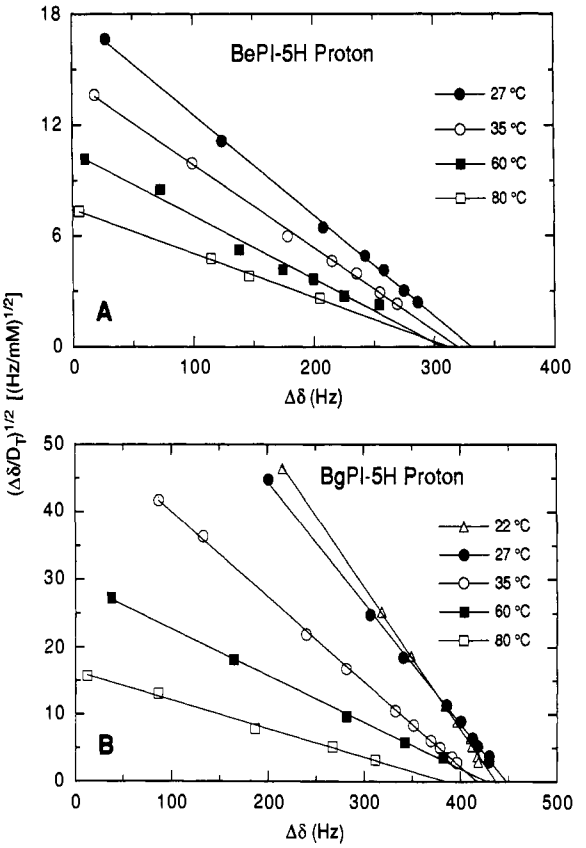

Figure 3. Plots of $(\Delta\delta/D_T)^{1/2}$ versus $\Delta\delta$ for the 5H aromatic protons of BePI (A) and BgPI (B) at the indicated temperatures in D_2O. Experimental conditions are the same as those stated in the legend of Figure 2.

Furthermore, self-association of BePI and BgPI should occur in such a way as to minimize the electrostatic repulsion from the two positive charges (on the pyridine rings and at the 3′-N positions of BePI and BgPI, see Figure 1) on each of the neighboring molecules. One possible model by which these repulsive forces would be minimized is one in which the ligand molecules successively stack together in alternating orientations, such that the aliphatic amino chain of each successive molecule in the *n*-mer is located on opposite sides of the stack. In such a case, the molecules might stack together to form a helical array.

Thermodynamics of Self-Association. Changes in the chemical shifts of the resonances corresponding to the aromatic protons of BePI and BgPI as a function of concentration were measured at different temperatures in order to characterize the dependency of the self-association binding constants on temperature. Plots of $(\Delta\delta/D_T)^{1/2}$ versus $\Delta\delta$ for the 5H aromatic protons of both BePI and BgPI at temperatures ranging from 22 to 80 °C are presented in Figure 3, parts A and B, respectively. The slopes of these plots decrease with increasing temperature. Thus, as one would expect since $K_a = x_0 s^2$, analysis of these plots with eq 1 yields association constants which decrease in magnitude with increasing temperature. A similar behavior was observed for all the other protons of both ligand molecules (data not shown). The self-association constants for both BePI and BgPI derived from the plots in Figure 3, as well as from those for the other aromatic protons (data not shown) except the 1H proton of BePI, are summarized in Table I. In addition, Table I presents the changes in free energy ($\Delta G°$) corresponding to these self-association constants, as calculated using the standard equation relating $\Delta G°$ and K_a:

$$\Delta G° = -RT \ln K_a \qquad (2)$$

Throughout the temperature range investigated, the self-association constants for BgPI are consistently greater than those

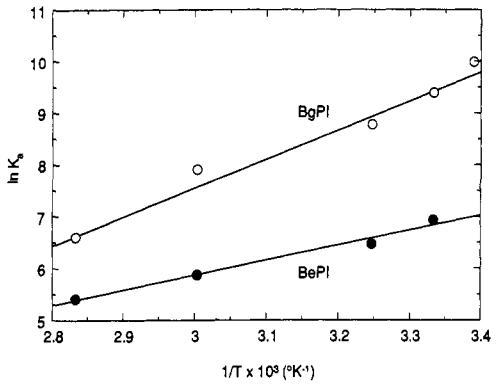

Figure 4. van't Hoff plot for the self-association interactions of both BePI (filled circles) and BgPI (open circles). Experimental conditions are the same as those stated in the legend of Figure 2.

Table II. Enthalpy and Entropy Changes for the Self-Association of BePI and BgPI[a]

ligand	$\Delta H°$ (kcal/mol)[b]	$\Delta S°$ (eu)
BePI	−5.7 ± 0.5	−5.6 ± 0.5
BgPI	−11.1 ± 0.4	−18 ± 0.7

[a] Determined from the van't Hoff plots in Figure 4 according to eq 3. Experimental conditions are the same as those stated in the footnote of Table I. [b] Mol refers to mole of self-associated complex formed.

for BePI, although the extent of this difference decreases with increasing temperature (K_a^{BgPI}/K_a^{BePI} = 12 at 27 °C and 3.4 at 80 °C). Thus, at temperatures ranging from 27 to 80 °C, BgPI has a higher self-affinity than BePI.

The self-association constants given in Table I for both BePI and BgPI are on the order of 10^2–10^4 M^{-1} at temperatures ranging from 22 to 80 °C. It should be pointed out that the total ligand concentrations used in the thermal denaturation, viscosity, and fluorescence studies ranged from 1.5 to 15 μM. Given these low concentrations and the self-association constants for BePI and BgPI listed in Table I, virtually all the ligand molecules were in their monomeric states for these experiments. Thus, self-association interactions were not interfering with those between the ligands and the DNA in these studies.

In order to determine the enthalpy and entropy changes ($\Delta H°$ and $\Delta S°$, respectively) for the self-association of BePI and BgPI, the data from Table I are plotted in Figure 4 according to the van't Hoff equation:

$$\ln K_a = -\frac{\Delta H°}{RT} + \frac{\Delta S°}{R} \qquad (3)$$

This equation postulates that plots of ln K versus $1/T$ will be linear, with their slopes and y-intercepts yielding values for $\Delta H°$ and $\Delta S°$, respectively. The $\Delta H°$ and $\Delta S°$ values derived from the plots in Figure 4 are listed in Table II. For the self-association interactions of both BePI and BgPI, the corresponding $\Delta S°$ values are negative (unfavorable), indicating that self-association is accompanied by a substantial entropic penalty. Negative (favorable) $\Delta H°$ values for the self-association of both BePI and BgPI indicate that these interactions are enthalpically driven and more than compensate for the entropic costs. This type of general thermodynamic behavior is consistent with that observed with other dimerizing dyes. The enhanced stability of the BgPI relative to the BePI self-associated complex is thus reflected by formation of the former complex corresponding to a negative $\Delta H°$ value (−11.1 kcal/mol) approximately twice that corresponding to formation of the latter complex ($\Delta H°$ = −5.7 kcal/mol).

Exchangeable Proton NMR Studies. Portions of the NMR spectra of BePI in 90% H_2O/10% D_2O at pH 5.0 and temperatures ranging from 0 to 30 °C are presented in Figure 5. The resonances corresponding to the 7-NH (10.9 ppm at 0 °C) and 11-NH (7.75 ppm at 0 °C) exchangeable protons (see Figure 1, left), as well those of all the aromatic protons, shift downfield as the temperature increases from 0 to 30 °C. Furthermore, the line widths of the exchangeable proton resonances increase with increasing temperature, with the converse applying to the aromatic proton resonances.

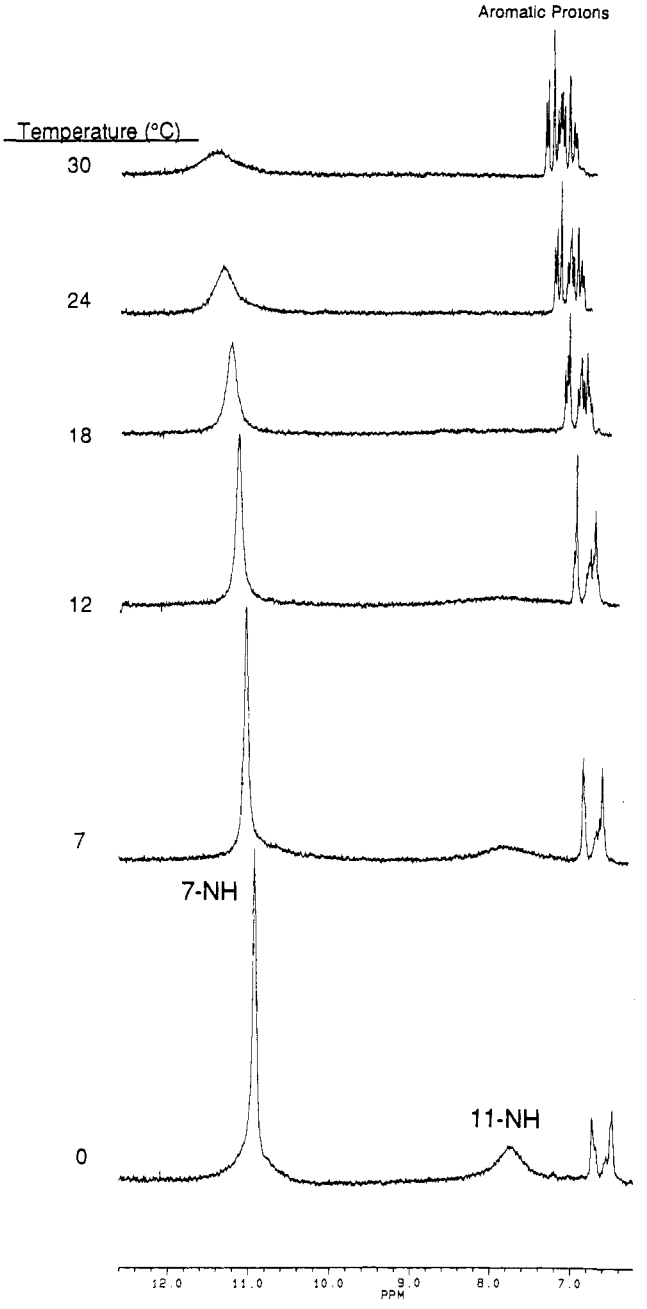

Figure 5. Portions of the proton NMR spectra of BePI in 90% H_2O/10% D_2O at the indicated temperatures. Buffer conditions are 10 mM sodium phosphate (pH 5.0) and 300 mM NaCl. The 7-NH, 11-NH, and aromatic proton resonances are indicated.

At any given temperature, a given BePI molecule is continually alternating between its monomeric and self-associated state, and the observed NMR spectrum at each temperature reflects an average over both states. In addition, the results in Figure 3 and Table II demonstrate that the self-association constant of BePI decreases with increasing temperature. Thus, as the temperature is raised, the ratio of self-associated to monomeric BePI decreases accordingly. The downfield shifts of the aromatic proton resonances with increasing temperature are consistent with this conclusion, as are their decreasing line widths, which reflect, in addition to a thermally-induced enhancement in tumbling rate,

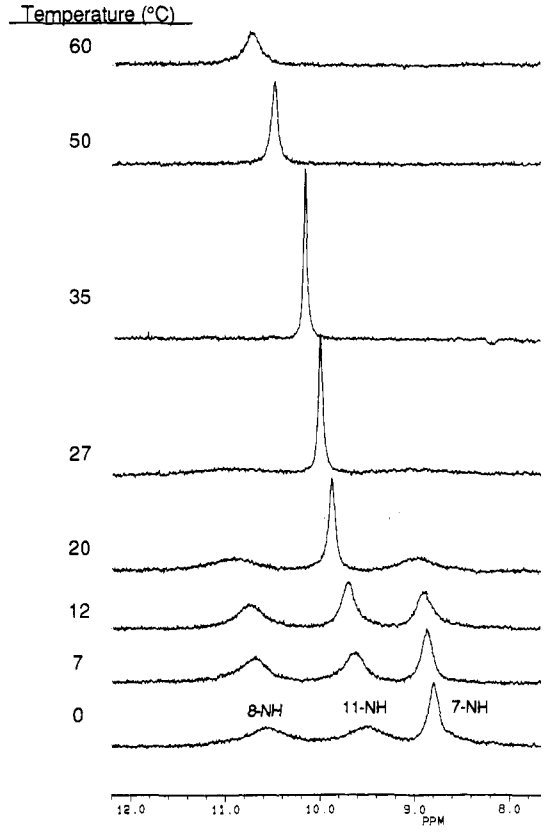

Figure 6. Portions of the proton NMR spectra of BgPI in 90% H_2O/10% D_2O at the indicated temperatures. Buffer conditions are the same as those stated in the legend of Figure 5. The 11-NH, 8-NH, and 7-NH exchangeable proton resonances are indicated.

the smaller hydrodynamic radii, and hence shorter correlation times (τ_c), of the monomeric relative to the self-associated form of BePI. The downfield shifts of the 7-NH and 11-NH exchangeable protons as a function of increasing temperature are also indicative of a decrease in the relative percentage of self-associated BePI, with $\Delta\delta$ values ($\approx$210 Hz) for the 7-NH and other aromatic protons approaching those observed for the aromatic protons in the D_2O NMR studies (Figure 2A).

The differences in chemical shifts between the 7-NH and 11-NH exchangeable proton resonances and that of H_2O (4.89 ppm) are approximately $\geq$900 Hz (3 ppm). These large differences in chemical shifts, coupled with the negligible changes in chemical shifts the 7-NH and 11-NH resonances undergo as a function of pH (Figure 7), indicate that these protons are under conditions of slow solvent exchange. By similar reasoning, the same may also be said for the 10-NH proton of BePI (see Figure 7), as well as the 11-NH, 7-NH, and 8-NH protons of BgPI (see Figures 6 and 8). Hence, any changes in the rates of solvent exchange, as indicated by the results in Figures 5, 6, 7, and 8, occur within those confines dictated by the conditions of slow exchange. The increasing line widths of the 7-NH and 11-NH resonances as a function of increasing temperature in Figure 5 reflect increasing solvent exchange rates. Solvent exchange rates of the NH protons in the self-associated form of BePI may be slower than those in the monomeric form, depending on the nature of the stacking interactions between neighboring molecules within the self-associated structure. In such a case, the observed increase in line width as a function of increasing temperature would reflect not only contributions from the thermally-induced enhancement in the rate of solvent exchange but the accompanying increase in the relative percentage of the monomeric form as well.

The resonance corresponding to the 10-NH proton of BePI partially overlaps that of the 7-NH proton (Figure 7A). Furthermore, the exchange rate of the 10-NH proton of BePI is quite rapid at pH 5.0 (see Figure 7A). This resonance is therefore only detectable as a small shoulder at the base of the 7-NH resonance in the 0 and 7 °C spectra of Figure 5.

Portions of the NMR spectra of BgPI in 90% H_2O/10% D_2O at pH 5.0 and temperatures ranging from 0 to 60 °C are presented in Figure 6. The resonances corresponding to the 8-NH (10.55 ppm at 0 °C), 11-NH (9.5 ppm at 0 °C), and 7-NH (8.8 ppm at 0 °C) exchangeable protons (see Figure 1, right) shift upfield as the temperature decreases from 60 to 0 °C. In addition, while the line width of the 7-NH resonance decreases with decreasing temperature, those of the 11-NH and 8-NH resonances decrease initially and then increase. Although not shown in Figure 6, the aromatic proton resonances also undergo upfield shifts in conjunction with decreasing temperature.

By the same reasoning described above for BePI, the results in Figure 6 are indicative of changes in the relative percentage of self-associated BgPI, with $\Delta\delta$ values ($\approx$400 Hz) for the 11-NH proton similar to those observed for the aromatic protons in the D_2O NMR studies (Figure 2B). As the temperature decreases, self-association increases, resulting in longer rotational correlation times and increasing line widths. However, decreasing temperatures are also accompanied by decreasing rates of solvent exchange, which result in decreasing line widths. As a consequence of these two opposite effects, decreasing temperatures are accompanied by initial decreases and subsequent increases in the line widths of the 11-NH and 8-NH resonances. This type of line width behavior is not exhibited by any of the NH resonances of BePI. At any given temperature, the ratio of self-associated to monomeric forms is higher for BgPI than for BePI (Table I). Thus, contributions to solvent exchange resulting from increases in this ratio are likely to be greater for BgPI than for BePI, which would account for the observed differences between the line width behaviors of the NH resonances of the two molecules.

In contrast to the 11-NH and 8-NH resonances of BgPI, the 7-NH resonance does not undergo an initial decrease and subsequent increase in line width with decreasing temperature. As briefly discussed above for BePI, this distinction may be due to stacking interactions between the heterocyclic ring portions of neighboring BgPI molecules in self-associated multimers. Both the 11-NH and 8-NH protons are ring protons, and may thus be engaged in close-range stacking interactions with other ring atoms of neighboring molecules, resulting in slow exchange rates. Conversely, the 7-NH proton is located in the aliphatic amino chain, and may thereby be less structurally constrained by such stacking interactions, thus exchanging more rapidly. In addition, the aliphatic amino chain is more mobile than the molecule as a whole (with a faster local correlation time) and may thus contribute to the differing behavior of the 7-NH resonance as well.

A comparison of Figures 5 and 6 reveals that, at 20 °C, the 7-NH and 8-NH resonances of BgPI (Figure 6) are broad but still detectable, whereas the corresponding 11-NH and 10-NH resonances of BePI are undetectable at 18 °C (Figure 5). Similarly, the line width of the 11-NH resonance of BgPI at 35 °C (Figure 6) is much narrower than that of the corresponding 7-NH resonance of BePI at 30 °C (Figure 5). These results would seem to indicate that the overall solvent exchange rates of the 11-NH, 7-NH, and 8-NH protons of BgPI are slower than those of the corresponding 7-NH, 11-NH, and 10-NH protons of BePI. However, these observed differences between the exchange rates of the NH protons of BePI and BgPI may be due to the latter having a higher ratio of self-associated to monomeric forms at any given temperature. NMR spectra of BePI and BgPI acquired at identical temperatures are therefore not directly comparable.

Solvent Exchange Rates of the NH Protons of BePI and BgPI. Changes in portions of the NMR spectra of BePI and BgPI in 90% H_2O/10% D_2O at either 0 °C (for BePI) or 35 °C (for

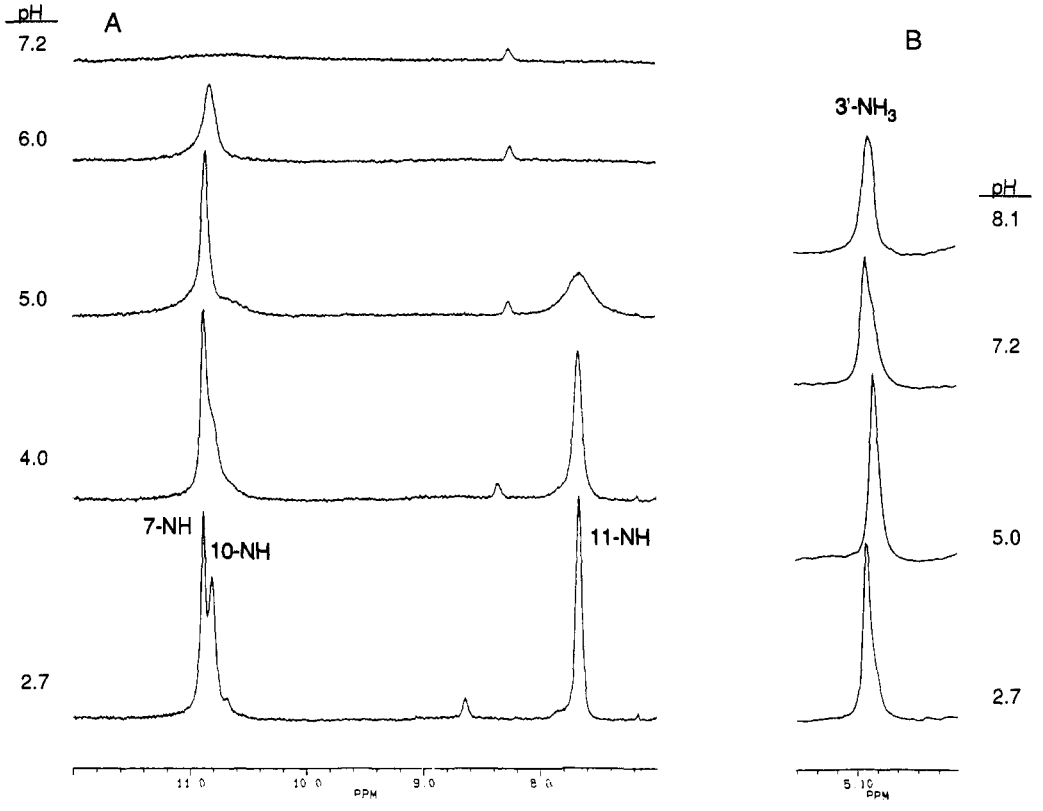

Figure 7. Portions of the proton NMR spectra of BePI in 90% H_2O/10% D_2O at the indicated pH values, showing the 7-NH, 10-NH, and 11-NH exchangeable proton resonances (A), as well as the 3′-NH_3 proton resonance (B). Buffer conditions are 10 mM sodium phosphate and 300 mM NaCl. The temperature is fixed at 0 °C. It should be noted that each division of the ppm scale is equal to 0.2 ppm in A but only 0.02 ppm in B.

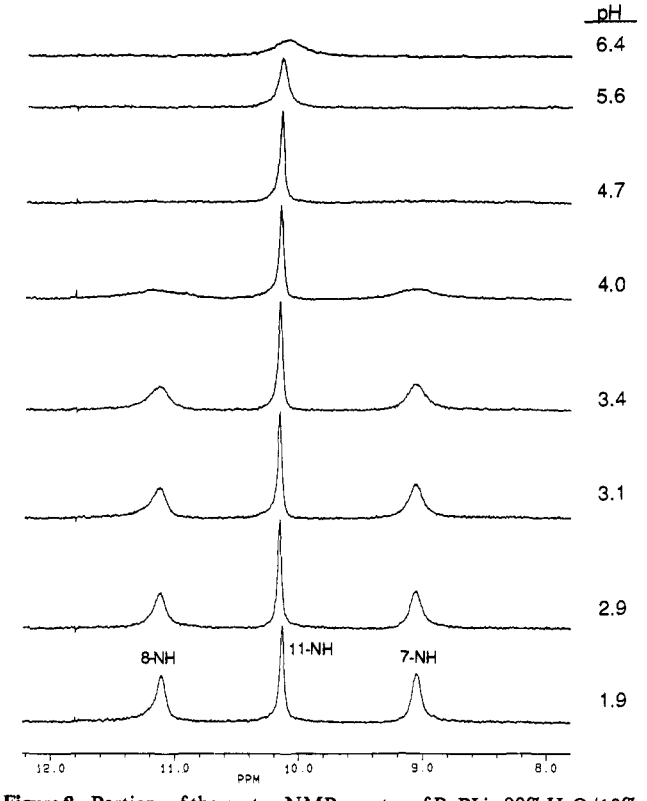

Figure 8. Portions of the proton NMR spectra of BgPI in 90% H_2O/10% D_2O at the indicated pH values, showing the 11-NH, 8-NH, and 7-NH exchangeable proton resonances. Buffer conditions are the same as those stated in the legend of Figure 7. However, the temperature is fixed at 35 °C.

BgPI) as a function of pH are shown in Figures 7 and 8, respectively. Raising the pH by addition of NaOH induces increases in the line widths of all the exchangeable proton resonances (7-NH, 11-NH, 8-NH, 10-NH, and/or 3′-NH), indicating increasing rates of solvent exchange. Furthermore, the chemical shifts of these resonances undergo slight upfield or no shifts with increasing pH, suggesting that the ratio of self-associated to monomeric forms changes very little, if any, throughout the pH range investigated. The 3′-NH resonance of BgPI overlaps the H_2O resonance and is therefore not observable.

From the van't Hoff plot in Figure 4, a K_a of 2.4×10^3 M^{-1} may be calculated for the self-association of BePI at 0 °C. Given this association constant, that for the self-association of BgPI at 35 °C (6.5×10^3 M^{-1}, see Table I), and the total BePI and BgPI concentrations used in the pH titrations (8.9 and 7.5 mM, respectively), the approximate percentage of self-associated ligand in each case may be estimated. These calculations reveal that roughly 80% of the BePI molecules and 85% of the BgPI molecules are self-associated under these experimental conditions. Hence, the relative exchange properties of the two molecules observed in these experiments are comparable to within approximately ±5%. The overall NaOH-induced solvent exchange rates (k_{ex}) for the exchangeable protons of BePI and BgPI were derived from the spectra in Figures 7 and 8, as well as from those acquired at other pH values (data not shown), according to the following equation:

$$k_{ex} = \frac{1}{T_{2+}} - \frac{1}{T_{2-}} \tag{4}$$

where T_{2-} is the T_2 relaxation time in the absence of exchange, derived from the NMR spectrum acquired in the absence of added NaOH (pH 1.6 for BgPI and 2.0 for BePI), and T_{2+} is the T_2 relaxation time in the presence of exchange (added NaOH). T_2 relaxation times were determined from the line widths of the

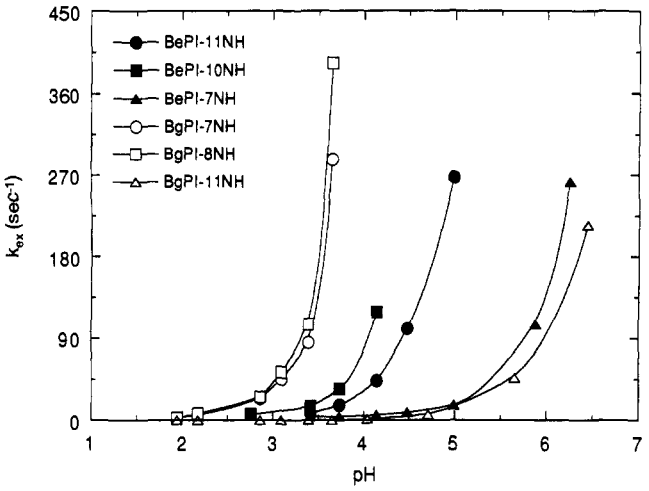

Figure 9. Changes in the solvent exchange rates of the NH protons of both BePI and BgPI as a function of pH. BePI data are presented as filled symbols, while BgPI data are presented as open symbols. Specific protons corresponding to each curve are as indicated. Buffer conditions are the same as those stated in the legend of Figure 7. The temperature was fixed at 0 °C for the BePI experiments and 35 °C for the BgPI experiments.

resonances according to the following relation:

$$\text{line width} = \frac{1}{\pi T_2} \tag{5}$$

Plots of the calculated k_{ex} values as a function of pH for the 7-NH, 11-NH, and 10-NH protons of BePI, as well as for the corresponding 11-NH, 7-NH, and 8-NH protons of BgPI, are shown in Figure 9. For each ligand, the rate of solvent exchange increases with increasing pH and does so in the following order: 10-NH > 11-NH ≫ 7-NH for BePI and 11-NH > 7-NH ≫ 8-NH for BgPI. Furthermore, at a given pH, the exchange rates of the 8-NH and 7-NH protons of BgPI are significantly faster than those of the corresponding 10-NH and 11-NH protons of BePI, while the exchange rate of the 11-NH proton of BgPI is similar to that of the corresponding 7-NH proton of BePI. These differences in observed solvent exchange rates may arise from differing intrinsic solvent exchange rates in the monomeric forms of the two ligands, as well as from structural differences between their self-associated complexes that affect the extent to which the exchangeable protons are involved in stacking interactions. As discussed above, the structural characteristics of BePI and BgPI allow for steric interactions between the 1H proton and the aliphatic amino chain (which includes the 11-NH proton) of the former, but not of the latter molecule. In either case, the 7-NH and 11-NH protons of BePI and BgPI, respectively, are unaffected, and, as experimentally observed, would therefore be likely to exchange with solvent protons to similar extents as a function of pH. In contrast, either the 11-NH and 10-NH protons of BePI or the corresponding 7-NH and 8-NH protons of BgPI would be affected by the presence of such steric interactions. The 7-N atom of BgPI, whose structure precludes the potential for any steric interactions, is able to achieve a normal electronic coupling with the pyridine ring, and thus with the 8-N atom. However, the presence of a steric interaction in BePI may alter this coupling, and hence the solvent exchange rates of the 11-NH and 10-NH protons.

Throughout the pH range (pH ≈ 2–8) indicated in Figures 7 and 9, the line width of the 3′-NH resonance of BePI barely increases, resulting in k_{ex} values ≤10 s^{-1}. This proton therefore exchanges much more slowly than any of the other exchangeable protons of BePI.

BePI and BgPI Preferentially Bind and Stabilize Triple-Helical DNA. Figure 10 demonstrates the effect of binding by either

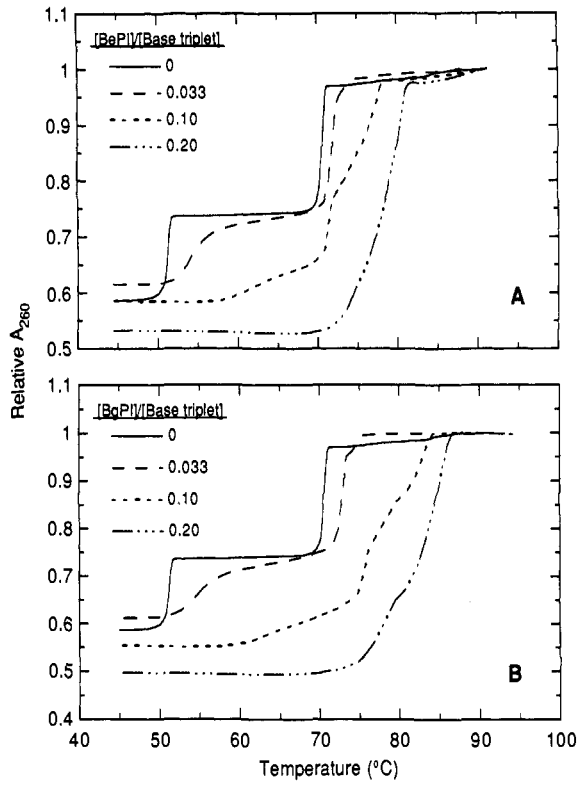

Figure 10. Thermal denaturation profiles for the poly(dA)·2poly(dT) triple helix in the presence or absence of either BePI (A) or BgPI (B). The [ligand]/[base triplet] ratios are as indicated. All the curves are normalized to an absorbance (at 260 nm) of 1 at 90 °C. The measured absorbances at 260 nm and 90 °C for the samples containing [ligand]/[base triplet] ratios of 0, 0.033, 0.10, and 0.20 are 1.019, 1.001 (BePI) or 1.012 (BgPI), 1.026 (BePI) or 1.130 (BgPI), and 1.118 (BePI) or 1.285 (BgPI), respectively. Base triplet concentrations were 40 μM, and CNE buffer was used in all experiments.

BePI (Figure 10A) or BgPI (Figure 10B) on the thermal stability of the poly(dA)·2poly(dT) triple helix. In the absence of ligand, the melting profile of the triplex is biphasic, with the first (lower-temperature) phase of the profile corresponding to the transition from triplex [poly(dA)·2poly(dT)] to duplex [poly(dA)·poly(dT)] plus single-stranded poly(dT) (Hoogsteen transition) and the second phase corresponding to dissociation of the remaining duplex [poly(dA)·poly(dT)] to single strands (Watson–Crick transition). However, in the presence of ligand, the melting profiles are either bi- (at a [ligand]/[base triplet] ratio of 0.2) or triphasic (at [ligand]/[base triplet] ratios of 0.033 and 0.1). The presence of more than two phases in some melting profiles reflects the ability of each ligand to shift from one binding site to another during the course of the melting transitions. In such a case, upon dissociation of a portion of the DNA helix, the ligands that were bound to that portion of the helix are released. These ligands are consequently available for binding to other sites on the remaining, nondissociated portion of the helix, thereby increasing the binding density, and hence thermal stability, of this helical region. This type of melting behavior is consistent with the ligand-binding theory proposed by McGhee (1976) for helix-stabilizing ligands.

For both BePI/poly(dA)·2poly(dT) and BgPI/poly(dA)·2poly(dT) complexes, the thermal stabilities of the triplexes increase by more than 20 °C as the [ligand]/[base triplet] ratio increases from 0 to 0.2 (near-saturating conditions), with BgPI enhancing triplex stability 2–3 °C more than BePI (compare Figure 10, parts A and B). This enhancement in thermal stability indicates that both ligands have higher binding affinities for the poly(dA)·2poly(dT) triplex than for the corresponding poly(dA)·poly(dT) duplex. It is interesting to note that the thermal stability of the Hoogsteen-paired, third strand is enhanced to a greater

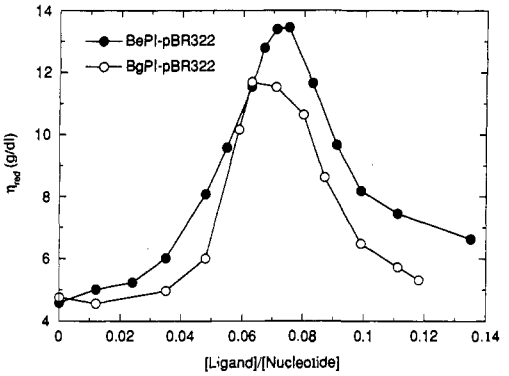

Figure 11. Reduced viscosities (η_{red}) of solutions containing either BePI/pBR322 or BgPI/pBR322 complexes as a function of the [ligand]/[nucleotide] ratio. Temperature was fixed at 24.5 ± 0.1 °C, and the buffer conditions are 10 mM tris·HCl (pH 7.1) and 1 mM EDTA.

extent between [ligand]/[base triplet] ratios of 0.1 and 0.2 than between ratios of 0 and 0.1. This effect suggests that both ligands bind the poly(dA)·2poly(dT) triplex in a cooperative manner. The T_m of the Watson–Crick transition increases by either ≈10 °C (for BePI/triplex, Figure 10A) or ≈14 °C (for BgPI/triplex, Figure 10B) as the [ligand]/[base triplet] ratio increases from 0 to 0.2, consistent with the results of control experiments on ligand/poly(dA)·poly(dT) complexes at [BePI or BgPI]/[base triplet] ratios ranging from 0 to 1 (data not shown). Thus, both ligands enhance the thermal stability of the poly(dA)·2poly(dT) triplex to a greater extent than that of the the poly(dA)·poly(dT) duplex. Previous studies[23–25] on short triple helices (14 base triplets in length) have indicated that the triplex specificities of both BePI and BgPI are not restricted to triplexes containing solely T×A·T base triplets, although strong binding occurs preferentially at T×A·T stretches.

BePI and BgPI Unwind Negatively-Supercoiled DNA. The effect of either BePI or BgPI on the viscosities of solutions containing pBR322 plasmid DNA is shown in Figure 11. As the [ligand]/[nucleotide] ratio increases, the viscosities of the plasmid solutions increase, reaching their maxima between ratios of 0.06 and 0.08, and then decrease to near starting levels. These viscosity changes correspond to the unwinding of the negatively-supercoiled plasmid to form a fully relaxed circular molecule (at the point of maximum viscosity), followed ultimately by formation of a postively-supercoiled molecule. This type of behavior has been previously observed by others in studies involving the interactions of intercalating ligands, such as EtBr, with supercoiled, circular DNA.[36–38] These results are therefore indicative of BePI and BgPI intercalation into circular, double-helical DNA. The BePI results confirm those previously reported by Pilch et al.[25]

Pilch and co-workers[25] have shown that binding by BePI increases the viscosities of solutions containing either double-helical or triple-helical polydeoxynucleotides, thereby suggesting that BePI intercalates into linear double-helical and triple-helical DNA. Viscosity studies in which BgPI was titrated into solutions containing either the poly(dA)·poly(dT) duplex or the poly(dA)·2poly(dT) triplex yielded similar results (data not shown), consistent with BgPI intercalation into linear double-helical and triple-helical DNA as well.

Binding to Double-Helical and Triple-Helical DNA Quenches the Fluorescence of Both BePI and BgPI. The fluorescence emission spectra of both BePI and BgPI, when free in solution or bount to either the poly(dA)·poly(dT) duplex or the poly(dA)·2poly(dT) triplex, are shown in Figure 12, parts A and B, respectively. Binding to both the duplex and the triplex substantially lowers the fluorescence intensities and quantum

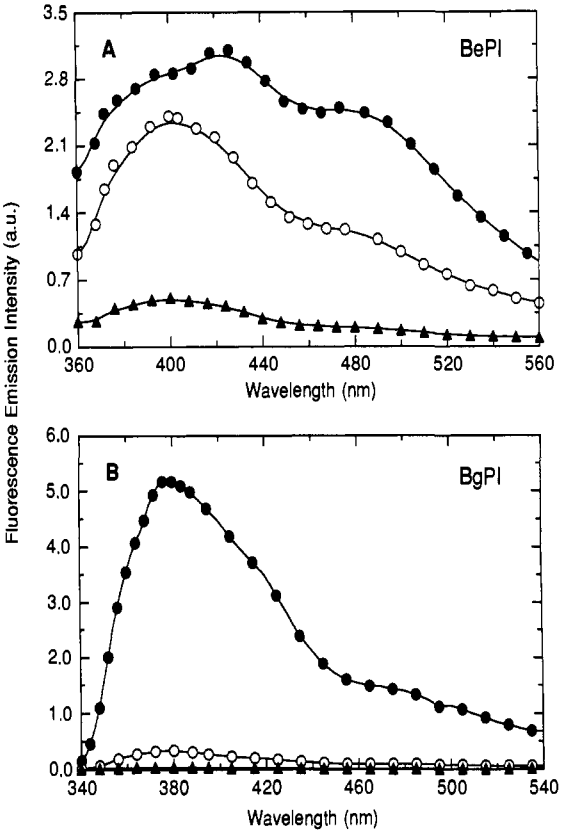

Figure 12. Fluorescence emission spectra of BePI (A) and BgPI (B), when free in solution (filled circles) or bound to either the poly(dA)·poly(dT) duplex (open circles) or the poly(dA)·2poly(dT) triplex (filled triangles). Solution conditions are 10 mM sodium cacodylate (pH 6.0), 300 mM NaCl, 0.1 mM EDTA, and 1.5 μM ligand. Excitation wavelengths are 315 and 280 nm for BePI and BgPI, respectively. For ligand/DNA complexes, the [base pair or base triplet]/[ligand] ratio is 14. The temperature was fixed at 25 °C.

Table III. Relative Fluorescence Quantum Yields of the Free and Bound Forms of BePI and BgPI[a]

sample	relative quantum yield[b]	relative I_{420}[c]
	BePI	
free BePI	1.0	1.0
BePI/poly[d(G-C)$_2$]	0.61	0.61
BePI/poly[d(A-T)$_2$]	0.81	0.63
BePI/poly(dA)·poly(dT)	0.61	0.71
BePI/poly(dA)·2poly(dT)	0.12	0.14
	BgPI	
free BgPI	1.0	1.0
BgPI/poly[d(G-C)$_2$]	0.045	0.039
BgPI/poly[d(A-T)$_2$]	0.034	0.028
BgPI/poly(dA)·poly(dT)	0.062	0.055
BgPI/poly(dA)·2poly(dT)	0.009	0.008

[a] Experimental conditions are the same as those stated in the legend of Figure 12. Excitation wavelengths are 315 and 280 nm for BePI and BgPI, respectively. In ligand/DNA complexes, the [base pair or base triplet]/[ligand] ratio is 14. [b] Fluorescence quantum yields were determined by integration of fluorescence emission spectra between wavelengths of either 370 and 560 nm for BePI or 340 and 525 nm for BgPI. [c] I_{420} is the fluorescence emission intensity at 420 nm. Fluorescence emission intensities were corrected to reflect an equal number of absorbed photons at the excitation wavelength.

yields of both ligands, with a markedly stronger quenching effect in BgPI/DNA relative to BePI/DNA complexes. Furthermore, binding to the triplex quenches the fluorescence of both ligands to a greater extent than binding to the duplex, with almost complete quenching of the BgPI fluorescence in the BgPI/triplex complex. Table III summarizes the relative quantum yields and fluorescence emission intensities at 420 nm of both BePI and BgPI, when free

(36) Crawford, L. V.; Waring, M. J. *J. Mol. Biol.* **1967**, *25*, 23–30.
(37) Bauer, W.; Vinograd, J. *J. Mol. Biol.* **1968**, *33*, 141–171.
(38) Keller, W. *Proc. Natl. Acad. Sci. U.S.A.* **1975**, *72*, 4876–4880.

in solution or bound to either the poly[d(A-T)$_2$], poly[d(G-C)$_2$], or poly(dA)·poly(dT) duplex, as well as to the poly(dA)·2poly-(dT) triplex. In each complex, the [base pair or base triplet]/[ligand] ratio is 14, and all corresponding fluorescence data are normalized relative to those for the free ligand (i.e. quantum yield or fluorescence emission intensity for the free ligand is set equal to 1). Under the conditions used in this study, binding to duplex DNA quenches the fluorescence of BePI and BgPI by averages of 32 and 95%, respectively, while binding to triplex DNA does so by 88 and 99%, respectively. The extent of stacking between the DNA bases and the intercalated ligands may be greater in the ligand/triplex relative to the ligand/duplex complexes. This differential degree of stacking may result in differences in the binding geometry between the two types of complexes, such that a stronger quenching effect is observed in the ligand/triplex complexes.

In addition to viscosity experiments, another method by which the mode of ligand binding may be characterized is through use of fluorescence excitation energy transfer experiments. Under identical experimental conditions to those used in this study, bases in the four BePI/polynucleotide complexes listed in Table III have been previously shown to transfer fluorescence excitation energy to bound BePI,[25] indicating that BePI was bound by intercalation in each complex. Unfortunately, it was not possible to carry out fluorescence energy transfer experiments on the BgPI/polynucleotide complexes due to their extremely low fluorescence quantum yields.

Conclusion

Both BePI and BgPI self-associate in solution, the latter doing so with a 3-fold (at 80 °C) to 12-fold (at 27 °C) higher affinity than the former. Self-association interactions do not interfere with those between either ligand and DNA at total ligand concentrations $\leq 10^{-5}$ M. Thermodynamic studies indicate that the self-association interactions are enthalpically driven, consistent with those of other dimerizing, aromatic dyes. Both exchangeable and nonexchangeable proton NMR experiments suggest that these interactions involve stacking interactions between aromatic ring groups. Both BePI and BgPI preferentially bind and stabilize triple-helical relative to double-helical DNA. Viscosity measurements are consistent with the conclusion that both ligands bind DNA by intercalation. Binding to DNA markedly quenches the fluorescence of both BePI and BgPI, with the greatest degree of quenching occurring upon binding to triplex relative to duplex DNA. Furthermore, the fluorescence of BgPI is quenched to a much greater extent than that of BePI upon binding to DNA.

Acknowledgment. We wish to thank Drs. Michel Rougée, Kalle Goering, and Jean-Louis Leroy for many helpful discussions. D. S. Pilch was supported by a Chateaubriand fellowship, awarded by the Ministère des Affaires Etrangères du Gouvernement Français.